Systematic study of exotic clustering in even-even actinide nuclei

B. Buck and A. C. Merchant
Department of Physics, University of Oxford, Theoretical Physics, 1 Keble Road, Oxford OX1 3NP, United Kingdom

S. M. Perez
Department of Physics, University of Cape Town, Private Bag, Rondebosch 7700, South Africa
(Received 22 April 1998)

We compare exotic cluster model predictions of the properties of 19 even-even actinide nuclei with experimental data. We restrict our attention to clusters which have been observed in exotic decay (i.e., ^{14}C, ^{20}O, ^{24}Ne, ^{28}Mg, and ^{32}Si) and concentrate on nuclei which may be modeled as Pb cores combined with these clusters, i.e., isotopes of Ra, Th, U, Pu, and Cm, respectively. Using fixed parameter values for all cases, we examine the energies of the states in the lowest $J^\pi=0^+,2^+,4^+,\ldots$ and $J^\pi=1^-,3^-,5^-,\ldots$ bands, the $B(E2\downarrow)$ transition strengths in the positive parity bands, and the values for $B(E3\uparrow;0^+\rightarrow3^-)$ and $B(E4\uparrow;0^+\rightarrow4^+)$. The level of agreement between calculated and measured values is generally good. [S0556-2813(98)00910-8]

PACS number(s): 21.60.Ev, 23.20.Lv, 23.70.+j, 27.90.+b

I. INTRODUCTION

We have previously found that a simple cluster model in which an alpha particle interacts with a core through a deep, local potential is capable of giving a good description of both the alpha decay half-lives of a wide range of nuclei [1,2] and of the detailed structure of those nuclei (^{20}Ne, ^{44}Ti, ^{94}Mo, and ^{212}Po) which can be described as a doubly magic core plus an alpha particle [3–5]. This cluster model was modified to describe exotic decay half-lives with equal success [6], reproducing also the main features of the low-lying states of those exotically decaying parent nuclei which could be described as a doubly magic ^{208}Pb core plus a ^{14}C, ^{20}O, ^{24}Ne, or ^{28}Mg cluster [7]. Further investigations involving a ^{14}C cluster combined with cores of ^{208,210,212}Pb [8] have provided an excellent description of many properties of the lowest $J^\pi=0^+,2^+,4^+,\ldots$ and $J^\pi=1^-,3^-,5^-,\ldots$ bands of the corresponding Ra isotopes, showing that it is not essential to have a core with a closed neutron shell. Most recently, a good account of the nuclei ^{232,234,236,238}U was also given in a study of the systems Pb + ^{24}Ne [9].

Here, we study all those actinide nuclei which can be described as binary systems involving a Pb core and one of the clusters emitted in exotic decay. In all, we examine 19 nuclei using a single cluster-core potential prescription. In the next section we briefly describe our cluster model. Then, in Sec. III, we compare calculated values of the energies of the states in the lowest positive and negative parity bands, the $E2$ transition strengths within these bands, and the $B(E3\uparrow;0^+\rightarrow3^-)$ and $B(E4\uparrow;0^+\rightarrow4^+)$ values with the experimental data for each set of isotopes. The level of agreement is good, and we present a few typical cases in greater detail. We also indicate the sort of parameter adjustment needed to bring the poorer examples into line with the data. In Sec. IV we examine systematic trends across the region of nuclei examined and the final section contains our conclusions.

We thus use our phenomenological model to investigate the consequences of assuming a substantial amount of exotic clustering in nuclei which have been observed to decay exotically. Independent justification for this assumption would be desirable, in particular from realistic microscopic calculations, but such calculations are not possible at present. We note, however, that a recent microscopic estimate [10,11] of the amount of alpha clustering in ^{212}Po results in a much larger value than hitherto supposed.

II. CLUSTER MODEL

For the even-even nuclei of interest here, our model postulates a cluster and a core in their 0^+ ground states interacting through a deep, local nuclear potential $V_N(r)$ and a Coulomb potential $V_C(r)$. The energies and wave functions of relative motion are obtained by solving the radial Schrödinger equation

$$\frac{-\hbar^2}{2\mu}\frac{d^2\chi_{nL}}{dr^2}+\left[\frac{\hbar^2L(L+1)}{2\mu r^2}+V_N(r)+V_C(r)\right]\chi_{nL}(r)=E_{nL}\chi_{nL}(r). \quad (1)$$

Physically acceptable solutions have the cluster nucleons in orbitals not already occupied by the core nucleons. This is roughly enforced by an appropriate choice of the quantum number $G=2n+L$ (see below), where n is the node number and L the orbital angular momentum of the state. Our model generates bands of states labeled by their common G value which will have positive parity and L values $0(2)G$ when G is even, and negative parity and L values $1(2)G$ when G is odd.

We then need to specify the value of G, as well as the form and parametrization of the nuclear potential, a not completely straightforward task. For a ^{208}Pb core, if we were describing the cluster and core nucleon orbitals by harmonic oscillator wave functions, with a common length parameter, the minimum possible value of G could be obtained by requiring all the cluster nucleons to occupy states above the

 © 1998 The American Physical Society

Fermi surface of the core. Thus, each proton orbital would have $2n_p+l_p=5$, and each neutron orbital $2n_n+l_n=6$. Summing the individual cluster nucleon contributions, and subtracting $G_{\rm int}$ associated with the shell model ground state structure of the cluster, would then lead to a well-defined value of $G=5Z_c+6N_c-G_{\rm int}$. Here Z_c and N_c are the numbers of protons and neutrons, respectively, in the cluster. When the valence protons and neutrons of the cluster occupy the same major shell (as they do for all the cases of interest here) we have $G_{\rm int}=Z_c+N_c-4=A_c-4$ for $2\leqslant(Z_c,N_c)\leqslant 8$ and $G_{\rm int}=2Z_c+2N_c-20=2A_c-20$ for $8\leqslant(Z_c,N_c)\leqslant 20$. Although the minimum acceptable values of G obtained in this way provide a useful guide, they are not rigorously applicable to heavy nuclei. In such systems the core and cluster have very different masses (and hence oscillator length parameters), and the spin-orbit force strongly shifts single-particle energies from harmonic shell values as well. Therefore, we treat G as a parameter which is expected to lie fairly close to the oscillator value, but which should actually be chosen so as to provide as good a description as possible of the data. Our studies of α clustering in heavy nuclei [1,2,5] suggest that the optimum value of G is intimately connected to the precise form of the nuclear potential, and that equally good descriptions of the available data may be made with slightly different values of G provided that compensatory adjustments are made in the nuclear potential parameters. This situation seems to prevail for exotic clustering as well, and so for simplicity and definiteness we make the global choice for the lowest allowed value of G for positive parity states of

$$G=5(Z_c+N_c)=5A_c, \tag{2}$$

for all clusters. This gives G values very close to the oscillator values for the lightest clusters of interest (70 for ^{14}C compared with an oscillator value of 68) and G values about 20% above this guideline for the heaviest clusters of interest (140 and 160 for ^{28}Mg and ^{32}Si compared with 120 and 134).

The choice of cluster-core nuclear potential is also not well determined, although some commonly used potential forms can be discarded as being unable to provide an acceptable simultaneous description of the exotic decay half-lives and the energies of the lowest bands. In particular, square wells and Woods-Saxon potentials with reasonable radii and diffusenesses, and also folded potentials obtained from reasonable density profiles and effective interactions (e.g., the M3Y potential), all yield inverted spectra. That is to say that the high-spin states have lower energies than the low-spin states, for the members of bands of both α and heavier clusters labeled by fixed values of G [5,12,13]. However, a simple analytic form for the cluster-core nuclear potential, involving a mixture of Woods-Saxon and cubed Woods-Saxon forms, has been found to give a good description of α clustering throughout the Periodic Table and of exotic clustering in a number of actinides [4,5,7], i.e.,

$$V_N(r)=-V_0\left[\frac{x}{1+\exp[(r-R)/a]}+\frac{1-x}{\{1+\exp[(r-R)/3a]\}^3}\right], \tag{3}$$

and in our first study of exotic cluster structure [7] we assigned the parameter values

$$T1:\quad V_0=56.6A_c\ \text{MeV},\quad a=0.75\ \text{fm},\quad x=0.36. \tag{4}$$

We note that these parameter values are very similar to those used in our studies of alpha clustering [4,5], with the dependence of the potential depth on cluster mass in line with a simple scaling of the nucleon-nucleus potential depth, as suggested by the folding model. We begin our systematic study of the actinides with these values for bands of positive parity states. The radius R must also be specified for a complete determination of the potential, and this is done by choosing it so as to reproduce the energy of one known state of the spectrum. We have usually chosen the 0^+ ground state for this purpose, but in view of this state's unique sensitivity to the potential in the nuclear interior, we feel that a better overall description can be achieved by fitting instead to the energy of the first excited 4^+ state.

Although Eqs. (2)–(4) represent the best overall potential prescription for exotic clustering we have found so far, there is certainly room for improvement. Indeed, for any nucleus where enough high quality data is available, we recommend the specific fitting of a potential, ideally by means of some of the inversion techniques presently being developed [14,15], in place of the global prescription given above (which may be regarded as a good starting point for such inversion procedures). Even the proposed parametrizations of Eqs. (2)–(4) contain ambiguities in the sense that modifications in one parameter value can usually be compensated by changes in the others to produce fits of very similar quality (such as the trade-off between the G value and the potential depth mentioned previously). It is, perhaps, too optimistic to expect that a single potential with fixed parameters can accurately describe such a diverse array of nuclei. Indeed, in our studies of ^{232,234,236,238}U [9] we found evidence for a small parity dependence in the potential depth (and radius) which shows up most clearly in the $B(E3\ \uparrow;0^+\rightarrow 3^-)$ values, as summarized in Sec. III C below. We dealt with this by taking $V_0^{(-)}=0.965V_0^{(+)}$ as the potential depth for negative parity states. We retain this modification in the following calculations, and also use a different value of the radius R for negative parity states, which we fix by fitting to the energy of the first excited 5^- state. Despite our reservations about the precise form of the potential, we do reproduce the available data rather well with the potential defined by Eqs. (2)–(4) for positive parity states, together with the modifications detailed above for negative parity states.

In addition to the nuclear cluster-core potential we also include a Coulomb potential appropriate to a point cluster interacting with a uniformly charged core with radius equal to that of the nuclear potential. Although more sophisticated treatments could be employed, their effects can be absorbed into the parameters adopted in the simpler case; so we use this for ease of calculation. With the G value and potential prescription thus determined, state energies and wave functions are obtained by solving the Schrödinger equation for the required values of L.

We shall also require $B(E2\ \downarrow)$ strengths within bands from an initial state $J_i=L$ to a final state $J_f=L-2$, which we calculate from

$$B(E2;J_i\rightarrow J_f)=\frac{\alpha_2^2}{4\pi}(2J_f+1)\langle J_f 0 J_i 0|20\rangle^2\langle r^2\rangle^2$$

$$=\frac{15\alpha_2^2}{8\pi}\frac{L(L-1)}{(2L+1)(2L-1)}\langle r^2\rangle^2, \qquad (5)$$

where $\langle r^2\rangle$ is the integral of the squared cluster-core separation distance r, multiplied by initial and final state radial wave functions, and in general, for multipolarity λ,

$$\alpha_\lambda=\frac{Z_1A_2^\lambda+(-1)^\lambda Z_2A_1^\lambda}{(A_1+A_2)^\lambda}, \qquad (6)$$

so that $\alpha_2=(Z_1A_2^2+Z_2A_1^2)/(A_1+A_2)^2$, with Z_i and A_i the charge and mass numbers of the cluster and the core. In some cases extensive $E2$ data are available from Coulomb excitation measurements, and are presented as the reduced matrix elements $\langle J_f||M(E2)||J_i\rangle$ rather than as $B(E2)$ strengths. The relation between these two quantities is a matter of definition via the Wigner-Eckart theorem, but the most common convention has

$$\langle J_f\|M(E2)\|J_i\rangle=\sqrt{B(E2\downarrow)\ \ [\text{in } e^2\,\text{fm}^4]\times(2J_i+1)}. \qquad (7)$$

In addition, we calculate $B(E3\uparrow;0^+\rightarrow 3^-)$ and $B(E4\uparrow;0^+\rightarrow 4^+)$ strengths for comparison with experiment. These are obtained from

$$B(E\lambda\uparrow;0^+\rightarrow\lambda)=\frac{2\lambda+1}{4\pi}\alpha_\lambda^2\langle r^\lambda\rangle^2 \quad e^2\,\text{fm}^{2\lambda}, \qquad (8)$$

where α_λ is defined in Eq. (6) above and $\langle r^\lambda\rangle^2$ replaces $\langle r^2\rangle^2$.

An effective charge ϵ may be introduced into the above expressions for electromagnetic transition strengths by changing Z_i to $Z_i+\epsilon A_i$, which corresponds to giving neutrons a charge of ϵe and increasing the proton charge to $(1+\epsilon)e$. The value of ϵ needed to obtain agreement with experimental $B(E2)$ transition strengths is typically in the range $0.2\leqslant\epsilon\leqslant 0.3$, indicating that our radial wave functions are not peaked sufficiently strongly at the nuclear surface. A more microscopically based treatment for ^{212}Po wave functions including both shell model and α-^{208}Pb cluster configurations confirms the need for such enhancements [10,11], and is a feature that it would be highly desirable to include eventually in our model.

We describe actinide nuclei in terms of a single cluster and core and concentrate on nuclei which can be modeled with an isotope of Pb as the core. The choice of cluster is guided by observations of exotic decay and the value of $B(E2\downarrow;2^+\rightarrow 0^+)$. The former strongly suggests a significant parentage of the emitted cluster in the ground state of the initial nucleus. Our model also produces values for $\langle r^2\rangle$ which are very similar for all the Pb-cluster combinations that we have examined. In the light of this, Eqs. (5) and (6) indicate that the measured values of $B(E2\downarrow;2^+\rightarrow 0^+)$ for a sequence of isotopes having a given cluster should be approximately equal to some constant which is characteristic of the cluster charge. Although the mass of the cluster is not so easily inferred, we expect the charge to mass ratio of the cluster to be similar to that of the core, to avoid setting up a large electric dipole moment (unobserved in practice). In line with these considerations, we restrict our attention to clusters which have been seen to be emitted in exotic decay, i.e., ^{14}C, ^{20}O, ^{24}Ne, ^{28}Mg, and ^{32}Si. We begin by using a cluster-core interaction defined by Eqs. (2)–(4), which we label potential $T1$ henceforth. Table I presents a comparison between the measured $B(E2\downarrow;2^+\rightarrow 0^+)$ values and those we calculate using an effective charge of $\epsilon=0.2e$ for the 19 nuclei of interest to us here. The jumps in the values between successive groups of isotopes are quite clear and produce strong support for the basic ideas of the cluster model. Although our calculations of $B(E2\downarrow;2^+\rightarrow 0^+)$ generally require a variation of the effective charge in the range $0.2\leqslant\epsilon\leqslant 0.3$ to bring them into *exact* agreement with the data, for definiteness we restrict ourselves to $\epsilon=0.2$ for all electromagnetic transitions in what follows. The next section examines the excited states of these isotopic sequences in more detail.

TABLE I. Values of $B(E2\downarrow;2^+\rightarrow 0^+)$ (W.u.).

System	Calculated ($\epsilon=0.2e$)	Experimental
^{220}Ra=^{14}C+^{206}Pb	94	—
^{222}Ra=^{14}C+^{208}Pb	91	111±9
^{224}Ra=^{14}C+^{210}Pb	88	97±4
^{226}Ra=^{14}C+^{212}Pb	85	123±5
^{226}Th=^{20}O+^{206}Pb	162	164±10
^{228}Th=^{20}O+^{208}Pb	162	167±6
^{230}Th=^{20}O+^{210}Pb	157	192±8
^{232}Th=^{20}O+^{212}Pb	152	198±11
^{234}Th=^{20}O+^{214}Pb	148	184±16
^{232}U=^{24}Ne+^{208}Pb	241	241±21
^{234}U=^{24}Ne+^{210}Pb	233	232±10
^{236}U=^{24}Ne+^{212}Pb	227	246±10
^{238}U=^{24}Ne+^{214}Pb	221	281±4
^{236}Pu=^{28}Mg+^{208}Pb	333	—
^{238}Pu=^{28}Mg+^{210}Pb	322	274±11
^{240}Pu=^{28}Mg+^{212}Pb	313	292±10
^{242}Pu=^{28}Mg+^{214}Pb	305	298.5±1.2
^{244}Pu=^{28}Mg+^{216}Pb	297	300±5
^{244}Cm=^{32}Si+^{212}Pb	411	415±25

III. SEQUENCES OF ISOTOPES

Using potential $T1$ and fixed effective charge $\epsilon=0.2$ we next present calculations for the energies of the states in the lowest $J^\pi=0^+,2^+,4^+,\ldots$ and $J^\pi=1^-,3^-,5^-,\ldots$ bands of our chosen nuclei, plus other observables [such as $B(E3\uparrow;0^+\rightarrow 3^-)$ and $B(E4\uparrow;0^+\rightarrow 4^+)$ strengths] wherever they have been directly measured (or, in the latter case, deduced from an overall fitting of the Coulomb excitation). A comparison of our calculated exotic decay half-lives with measured values can be found in Table I of Ref. [7]. We supplement these calculations by using modified potentials when deviations from the observed excitation energies warrant an effort to improve the theoretical description. To this

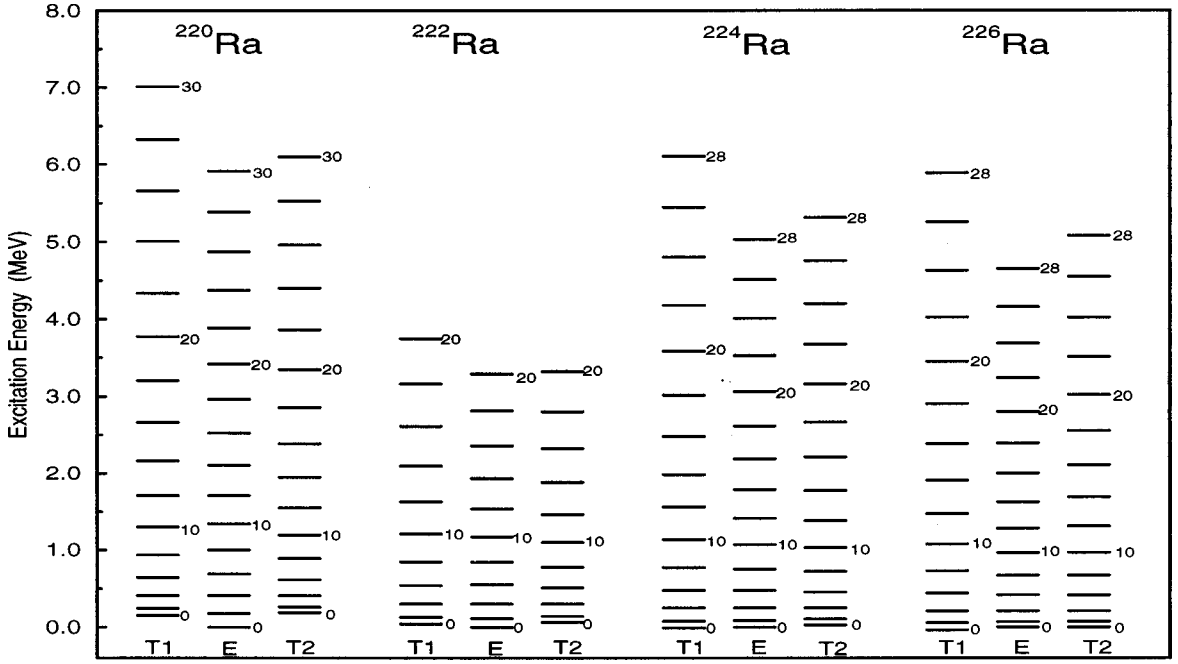

FIG. 1. Comparison of energies calculated using potentials $T1$ and $T2$ with experiment for the lowest band of positive parity states in ^{220,222,224,226}Ra.

end we define two further sets of parameter values:

$$T2: \quad V_0^+ = 53.9A_c \ \text{MeV}, \quad a = 0.73 \ \text{fm}, \quad x = 0.36 \tag{9}$$

and

$$T3: \quad V_0^+ = 59.6A_c \ \text{MeV}, \quad a = 0.77 \ \text{fm}, \quad x = 0.36, \tag{10}$$

labeling the corresponding potentials by $T2$ and $T3$, respectively. Both $T2$ and $T3$ yield good fits to the exotic decay half-lives of Table I of Ref. [7], with $T2$ having been used previously in calculating the properties of isotopes of Ra and U [8,9]. In all cases we continue to use $G = 5A_c$ and $V_0^- = 0.965V_0^+$. The successively higher values of the diffuseness a for the potentials $T2$, $T1$, and $T3$ lead to progressively more stretched-out spectra (smaller effective moments of inertia). The main effect of using these different potentials is thus on the excitation energies of the higher-spin states, with those of the low-spin values scarcely affected and the effect on the electromagnetic transition rates marginal. One common fault is that often we do not describe the 0^+-2^+-4^+ or the 1^--3^--5^- spacings very well, indicating that our potential does not have quite the right shape near the origin. This is also borne out by its having a nonzero derivative at $r = 0$, and so in principle, there is room for some improvement. Nevertheless, the global fit to the excitation energies of 19 different nuclei using the fixed parameter values of potential $T1$ of Eqs. (2)–(4) is surprisingly good and, even in the worst cases, is superior to that obtained from a rigid rotor with moment of inertia based on the 0^+–2^+ spacing. Furthermore, we reproduce rather well many of the electromagnetic properties of these nuclei using a consistent approach with a single (moderate) value of the effective charge throughout.

A. ^{220,222,224,226}Ra = ^{14}C + ^{206,208,210,212}Pb

Figures 1 and 2 compare our results using potential $T1$ for the energies of the lowest positive and negative bands of states in ^{220,222,224,226}Ra with the experimental values [16–20]. The experimental database for ^{222,224}Ra has recently been enlarged by Cocks *et al.* [16]. The calculated bands are stretched out a little too much, generally overestimating the energy of the state of highest known spin in each isotope by up to 1 MeV. The experimental tendency for I to increase slightly as the core mass increases (compare the energies of the 20^+ states of the various isotopes, for example) is correctly reproduced.

The problem with the moments of inertia has been noted before [8], and can be largely corrected by using a potential with a slightly smaller diffuseness (and smaller depth). A previous study [8] used potential $T2$ to calculate the properties of ^{222,224,226}Ra, and in Figs. 1 and 2 we also reproduce the improved fit to the excitation energies obtained with this potential.

A thorough discussion of the electromagnetic data available for ^{222,224,226}Ra, and our model's success in describing it with the parameters of potential $T2$, is given in Ref. [8]. Since our predictions for electromagnetic properties are largely insensitive to the choice of potential, and since no extra data are available for ^{220}Ra, we simply summarize our previous results. For ^{226}Ra, using an effective charge of $0.25e$, we were able to give a good account of the $E2$ and $E3$ transition rate data obtained from Coulomb excitation measurements by Wollersheim *et al.* [21] involving many states of both bands. We also gave a satisfactory account of the $B(E2\uparrow;0^+\rightarrow 2^+)$, $B(E3\uparrow;0^+\rightarrow 3^-)$, and $B(E4\uparrow;0^+\rightarrow 4^+)$ transition strengths. The only difficulty encountered was in describing the $E1$ transition rates. The electric dipole operator is uniquely sensitive to the neutron/proton ratios in the cluster and core, and could not be accu-

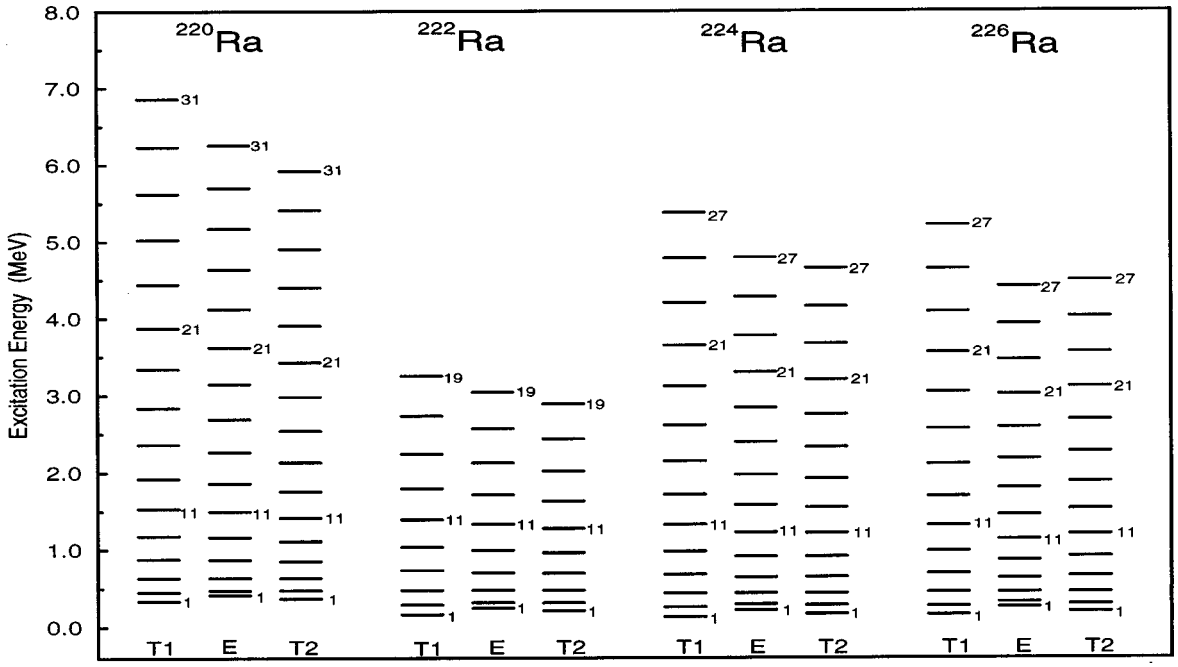

FIG. 2. Comparison of energies calculated using potentials $T1$ and $T2$ with experiment for the lowest band of negative parity states in ^{220,222,224,226}Ra.

rately deduced from a single cluster-core combination. A superposition of several cluster-core pairs, centered on the combination used in the simple model, is almost certainly necessary. However, it was possible to circumvent this complication by fitting the electric dipole moment to the data (which required the introduction of one extra parameter). Then the $E1$ transitions in ^{226}Ra could be well described by the model. A similar strategy was also successful in describing the measurements of $B(E1\downarrow)/B(E2\downarrow)$ ratios in ^{222}Ra and ^{224}Ra [16]. An excellent account of the exotic decay half-lives for ^{14}C emission from ^{222,224,226}Ra was obtained from the parameter sets of both potential $T1$ and potential $T2$.

B. ^{226,228,230,232,234}Th = ^{20}O + ^{206,208,210,212,214}Pb

Calculated and experimental spectra for ^{226,228,230,232,234}Th [22–25] are shown in Figs. 3 and 4. In terms of our systematic investigation of trends from the Ra to Cm isotopes, these nuclei represent a changeover region.

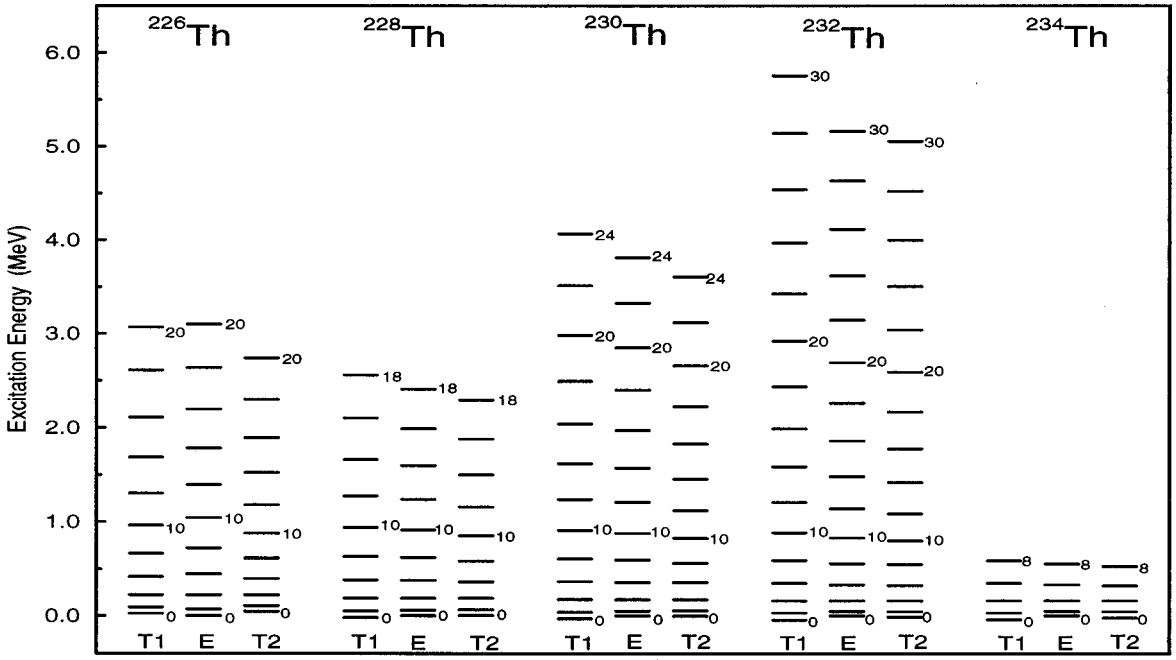

FIG. 3. Comparison of energies calculated using potentials $T1$ and $T2$ with experiment for the lowest band of positive parity states in ^{226,228,230,232,234}Th.

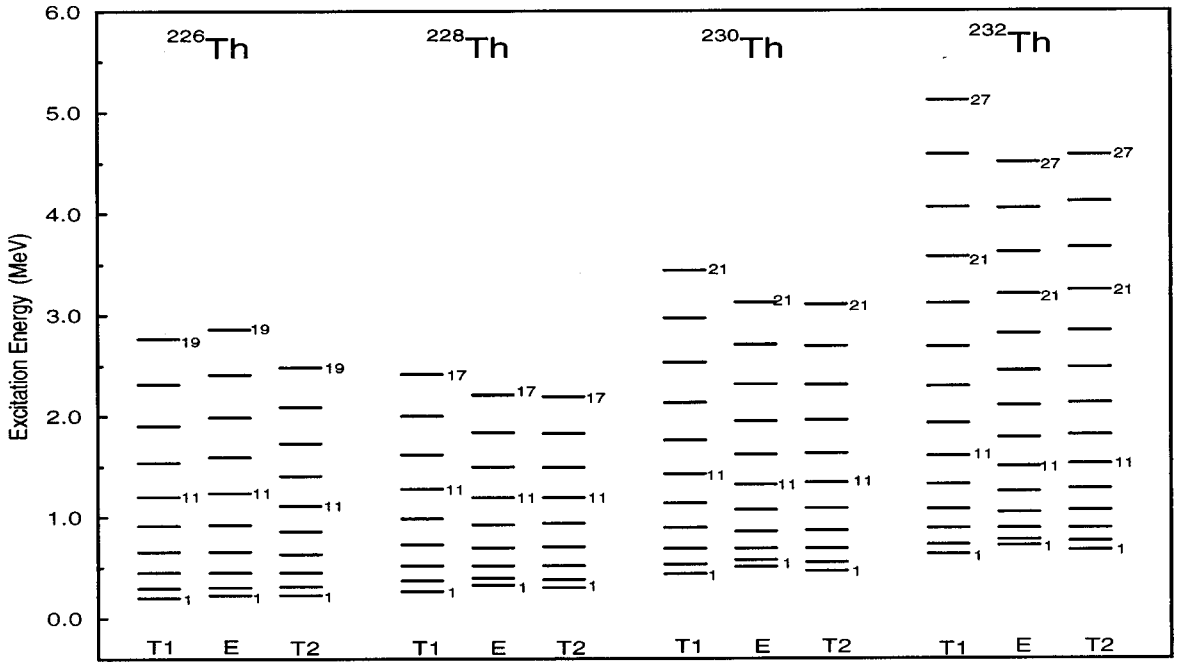

FIG. 4. Comparison of energies calculated using potentials $T1$ and $T2$ with experiment for the lowest band of negative parity states in ^{226,228,230,232,234}Th.

In the Ra isotopes, the parameters of potential $T2$ generally provide a superior fit to those of $T1$, whereas from the U isotopes onward, the parameters of potential $T1$ give better results. However, for the above-mentioned Th isotopes, some are best described with $T1$, others by $T2$, and some fall almost midway between the two sets of calculations. The figures show that both the positive and negative parity energies of ^{226}Th are very well accounted for by $T1$, even at the lowest-spin values, so that this calculation represents one of our more successful reproductions of the experimental data in the actinide region. However, the measured energies of the positive parity states of ^{228}Th lie between $T1$ and $T2$ (and could be best described by a potential having diffuseness $a=0.74$ fm), whereas the negative parity states are very well described by $T2$. For ^{234}Th only positive parity states up to 8^+ are presently known, and this limited information is adequately described by both $T1$ and $T2$. Our description of ^{230}Th is of about the same standard as that of ^{228}Th. Thus, the experimental positive parity states generally lie between the predictions of $T1$ and $T2$, whereas the experimental negative parity states are well described by T2. In ^{232}Th, however, both positive and negative parity states are best described by $T2$, which gives rise to another of the more successful applications of our model to the actinide nuclei.

There are measurements of $B(E2\downarrow;2^+\rightarrow 0^+)$ based on lifetime measurements for ^{226,228,230,232,234}Th. The values are close enough to each other to suggest that the dominant cluster is an isotope of O in all cases, but the effective charges required to reproduce the measured values exactly [$\sim 0.2e$ for ^{226,228}Th and $\sim(0.26-0.29)e$ for ^{230,232,234}Th] again indicate some small change between these sets of isotopes. Additional lifetime data for ^{228,230}Th allow values of $B(E2\downarrow;4^+\rightarrow 2^+)$ to be deduced of 242 ± 9 and 261 ± 11 Weisskopf units (W.u.), respectively. Our calculations using $\epsilon=0.20e$ yield 231 and 224 W.u. for comparison.

In addition to $E2$ transition strengths, directly measured values of $B(E3\uparrow;0^+\rightarrow 3^-)$ and inferred values of $B(E4\uparrow;0^+\rightarrow 4^+)$ are also available for ^{230,232}Th. Our calculated values, using Eqs. (6) and (8) and an effective charge of $\epsilon=0.2e$, are shown in Tables II and III. The $E3$ transitions are very well described by our model, and the calculated $E4$ results are also in acceptable agreement with experiment.

As a final point, it is interesting to note that there are indications of exotic cluster structure in the thorium isotopes in addition to the ^{20}O-Pb combination studied here. The observation that ^{230}Th can decay by emitting ^{24}Ne [26] suggests that it may contain a significant ^{24}Ne–^{206}Hg component, which might be correlated with the spectral changes between ^{226,228}Th and ^{230,232}Th noted above. Also, the observed $B(E2\downarrow;2^+\rightarrow 0^+)$ strengths of 74 ± 7 and 96 ± 7 observed in ^{222}Th and ^{224}Th, respectively, are characteristic of values obtained with ^{14}C clusters. The spectra of these two nuclei can also be reasonably well modeled as ^{14}C-Po systems with a potential in line with Eqs. (2)–(4). Although we do not pursue the idea further here, we note that these indications suggest that the dominant exotic cluster may be changing as the thorium isotopes are traversed from $A=222$ to 234.

C. ^{232,234,236,238}U=^{24}Ne+^{208,210,212,214}Pb

Figures 5 and 6 present a comparison of the observed lowest positive parity and negative parity bands of ^{232,234,236,238}U [24,25,27] with the results of a ^{24}Ne $+^{208,210,212,214}$Pb cluster model using potential $T1$, as well as with the results of an earlier calculation [9,28] using potential $T2$. The experimental energies for ^{232}U are quite tightly sandwiched between the values calculated from these two prescriptions, while the spectra of ^{236}U and ^{238}U are best described by $T1$. The energy levels of ^{234}U are very well fitted with potential $T2$ [28].

TABLE II. Values of $B(E3\uparrow;\ 0^+\rightarrow 3^-)\ e^2\,\mathrm{b}^3$

System	Calculated ($\epsilon=0.2e$)	Experimental [21,29]
$^{226}\mathrm{Ra}=^{14}\mathrm{C}+^{212}\mathrm{Pb}$	0.63	0.74 ± 0.04 and 1.10 ± 0.11
$^{230}\mathrm{Th}=^{20}\mathrm{O}+^{210}\mathrm{Pb}$	0.68	0.64 ± 0.06
$^{232}\mathrm{Th}=^{20}\mathrm{O}+^{212}\mathrm{Pb}$	0.63	0.65 ± 0.06 and 0.45 ± 0.05
$^{234}\mathrm{U}=^{24}\mathrm{Ne}+^{210}\mathrm{Pb}$	0.67	0.50 ± 0.18
$^{236}\mathrm{U}=^{24}\mathrm{Ne}+^{212}\mathrm{Pb}$	0.62	0.53 ± 0.07 and 0.69 ± 0.08
$^{238}\mathrm{U}=^{24}\mathrm{Ne}+^{214}\mathrm{Pb}$	0.58	0.59 ± 0.05 and 0.64 ± 0.06
$^{238}\mathrm{Pu}=^{28}\mathrm{Mg}+^{210}\mathrm{Pb}$	0.58	0.71 ± 0.12
$^{240}\mathrm{Pu}=^{28}\mathrm{Mg}+^{212}\mathrm{Pb}$	0.53	0.41 ± 0.06
$^{242}\mathrm{Pu}=^{28}\mathrm{Mg}+^{214}\mathrm{Pb}$	0.48	0.42 ± 0.07
$^{244}\mathrm{Pu}=^{28}\mathrm{Mg}+^{216}\mathrm{Pb}$	0.43	0.30 ± 0.10
$^{244}\mathrm{Cm}=^{32}\mathrm{Si}+^{212}\mathrm{Pb}$	0.44	0.52 ± 0.07

There are extensive measurements on the $E2$ transitions rates within the positive parity bands of ^{234,236,238}U, coming mainly from Coulomb excitation experiments [31–35]. The results of calculations of these electromagnetic quantities are largely independent of which potential parameter set we use, and we have already given a good account of the reduced $E2$ matrix elements for ^{234,236,238}U for spin values 0^+–28^+, 0^+–28^+ and 0^+–30^+ using potential $T2$ and effective charges of $0.2e$, $0.2e$, and $0.25e$, respectively, in Table III of Ref. [9].

There are also direct measurements of $B(E3\uparrow;0^+\rightarrow 3^-)$ and deduced values of $B(E4\uparrow;0^+\rightarrow 4^+)$ available for ^{234,236,238}U. The $E3$ strengths give a very strong indication that a small parity dependence is needed in the cluster-core potential [9]. We have introduced this by taking a potential depth V_0^- for the negative parity states, which is 96.5% of the depth V_0^+ for the positive parity states, and using a different value for the potential radius fitted to place the lowest excited 5^- at the correct energy. This radius is a little larger than that for the positive parity states, resulting in the moment of inertia for the negative parity band being a little larger than that for the positive parity band, an effect observed in many of the isotopes examined to date. The parity dependence of the potential leads to a phase difference between the oscillations of the radial wave functions of the positive and negative parity states involved in an $E3$ transition, which in turn leads to a reduced transition strength [9]. Failure to account for this effect leads to repeated overestimates of $B(E3\uparrow;0^+\rightarrow 3^-)$ by a factor 6–7. Table II shows that, with this adjustment, a good account can then be given of values of $B(E3\uparrow;0^+\rightarrow 3^-)$, not just for ^{234,236,238}U, but also for other actinide nuclei. Table III shows that we also achieve a fair reproduction of the $B(E4\uparrow;0^+\rightarrow 4^+)$ strengths, although we are not able to account for the small

TABLE III. Values of $B(E4\uparrow;\ 0^+\rightarrow 4^+)\ e^2\,\mathrm{b}^4$.

System	Calculated ($\epsilon=0.2e$)	Experimental [21,30]
$^{226}\mathrm{Ra}=^{14}\mathrm{C}+^{212}\mathrm{Pb}$	1.10	1.08 ± 0.15
$^{230}\mathrm{Th}=^{20}\mathrm{O}+^{210}\mathrm{Pb}$	1.83	1.19 ± 0.32
$^{232}\mathrm{Th}=^{20}\mathrm{O}+^{212}\mathrm{Pb}$	1.79	1.48 ± 0.34
$^{234}\mathrm{U}=^{24}\mathrm{Ne}+^{210}\mathrm{Pb}$	2.63	1.96 ± 0.56
$^{236}\mathrm{U}=^{24}\mathrm{Ne}+^{212}\mathrm{Pb}$	2.57	1.69 ± 0.57
$^{238}\mathrm{U}=^{24}\mathrm{Ne}+^{214}\mathrm{Pb}$	2.53	0.69 ± 0.37
$^{238}\mathrm{Pu}=^{28}\mathrm{Mg}+^{210}\mathrm{Pb}$	3.49	1.9 ± 0.7
$^{240}\mathrm{Pu}=^{28}\mathrm{Mg}+^{212}\mathrm{Pb}$	3.42	1.3 ± 0.6
$^{242}\mathrm{Pu}=^{28}\mathrm{Mg}+^{214}\mathrm{Pb}$	3.36	$0.55^{+0.53}_{-0.41}$
$^{244}\mathrm{Pu}=^{28}\mathrm{Mg}+^{216}\mathrm{Pb}$	3.30	$0.09^{+0.55}_{-0.09}$
$^{244}\mathrm{Cm}=^{32}\mathrm{Si}+^{212}\mathrm{Pb}$	4.32	$0.0^{+0.25}_{-0.0}$

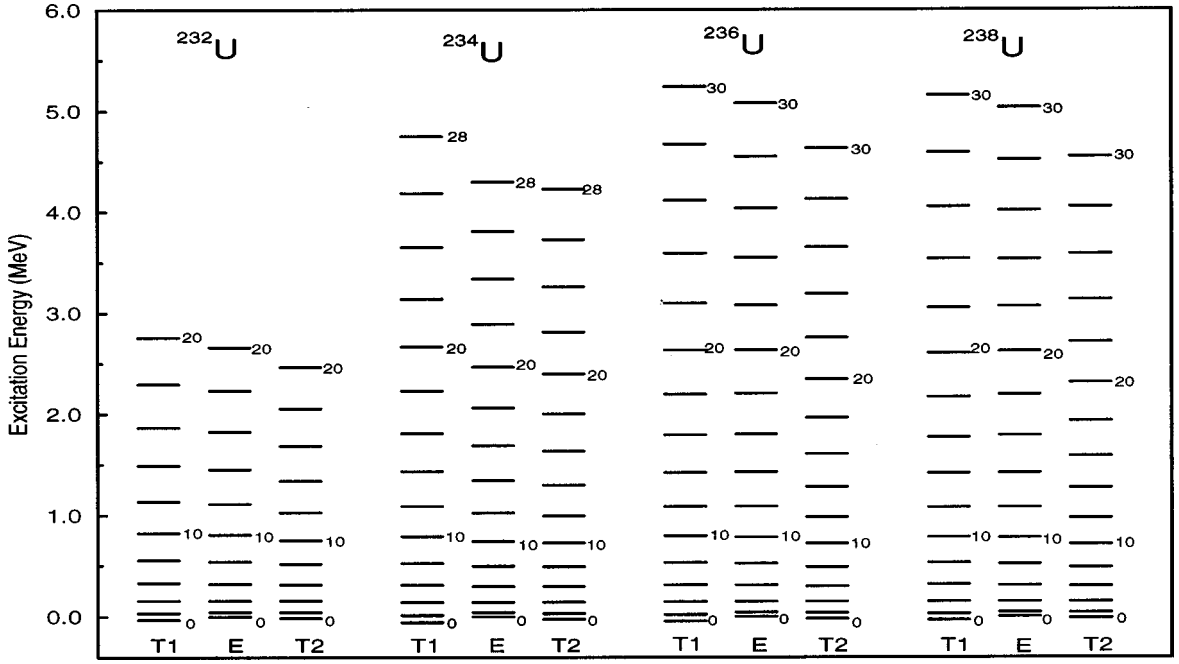

FIG. 5. Comparison of energies calculated using potentials $T1$ and $T2$ with experiment for the lowest band of positive parity states in ^{232,234,236,238}U.

value deduced for ^{238}U. Good descriptions of the half-lives for ^{24}Ne emission from ^{232,234}U are also achieved with the parameter sets of both $T1$ [7] and $T2$ [9].

D. ^{236,238,240,242,244}Pu=^{28}Mg+^{208,210,212,214,216}Pb

Figure 7 compares our calculations of the energies of the bands of lowest-lying positive parity states of $^{236-244}$Pu using potential $T1$, with the currently available data [24,27,36–39]. Apart from the usual difficulties in describing the 0^+-2^+ spacings, the lower reaches of the spectra are well reproduced up to spins of about 10^+. In the heavier isotopes ^{242,244}Pu, there are indications, even for these low-spin states, that the calculations are underestimating the energies. This problem gets progressively worse for higher spins, and the values for the 26^+ states in ^{242,244}Pu are about 0.4 MeV below the measured values. A modification of the parameters to the values for $T3$ given in Eq. (10) corrects this problem. We plot the resulting spectra in Fig. 7, labeled by $T3$. The calculated energies of the states in the lighter isotopes $^{236-240}$Pu are now slightly overestimated, but those of

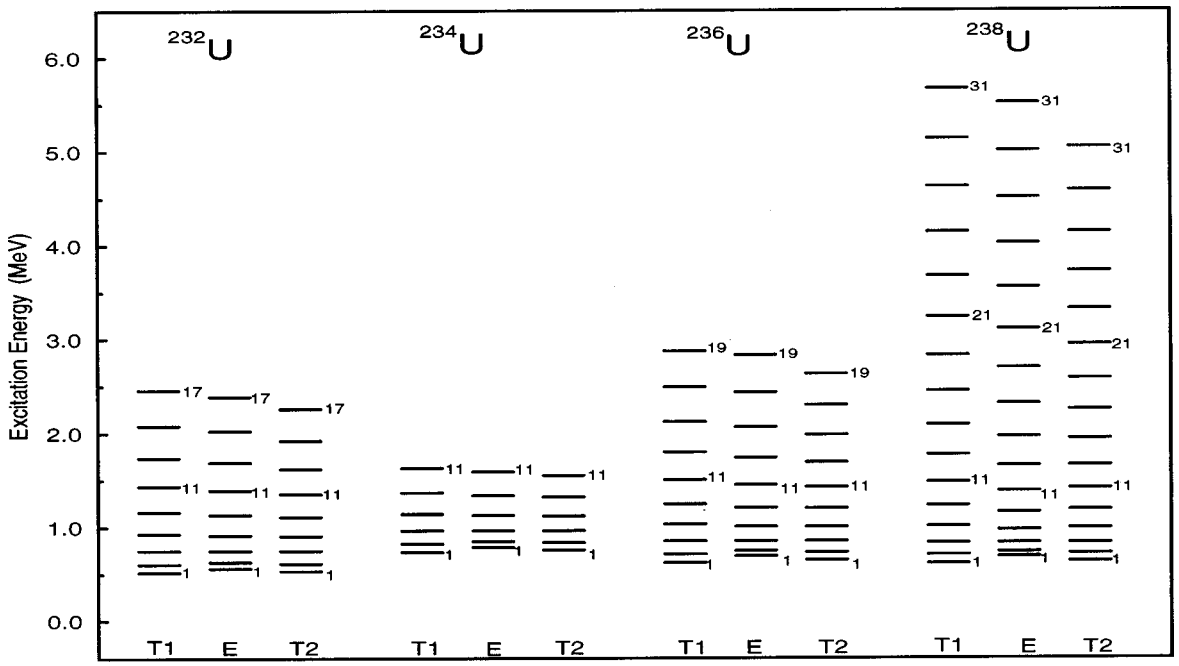

FIG. 6. Comparison of energies calculated using potentials $T1$ and $T2$ with experiment for the lowest band of negative parity states in ^{232,234,236,238}U.

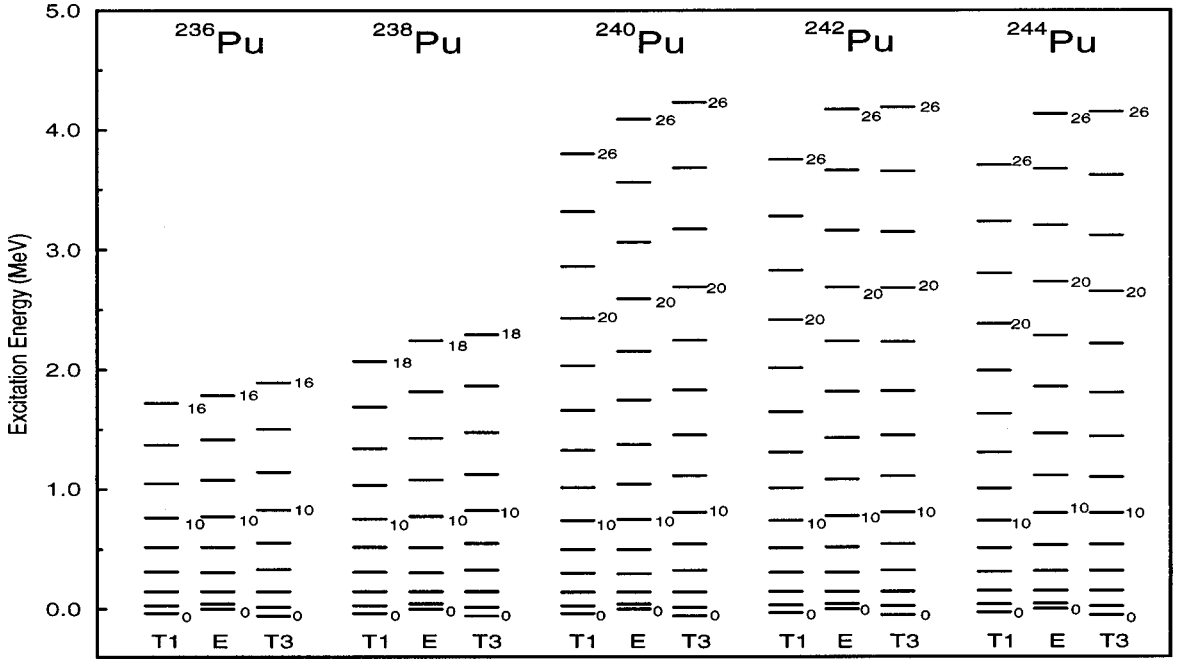

FIG. 7. Comparison of energies calculated using potentials $T1$ and $T3$ with experiment for the lowest band of positive parity states in ^{236,238,240,242,244}Pu.

^{242,244}Pu are much improved, so much so, that the spectrum for ^{242}Pu represents one of the best fits we have been able to achieve.

Energies of negative parity states in ^{236,238,242,244}Pu have not been measured beyond the 1^--3^--5^- states, and so no spectra are plotted for these cases. However, negative parity states in ^{240}Pu have recently been reported [37] up to $J^\pi = 27^-$, and we compare calculations using potentials $T1$ and $T3$ with these measurements in Fig. 8. The results from $T1$ are in very good agreement with the data, while the energies from $T3$ are slightly larger. There is not a great deal of information on the electromagnetic transitions in these nuclei, and Tables I and II show that the calculated $B(E2\downarrow; 2^+ \rightarrow 0^+)$ are all in satisfactory agreement with measurements. The only significant deviations are those exhibited by the $B(E4\uparrow; 0^+ \rightarrow 4^+)$ strengths deduced from Coulomb excitation experiments for $^{238\text{-}244}$Pu [30], which are seen to decrease with increasing mass number and, for

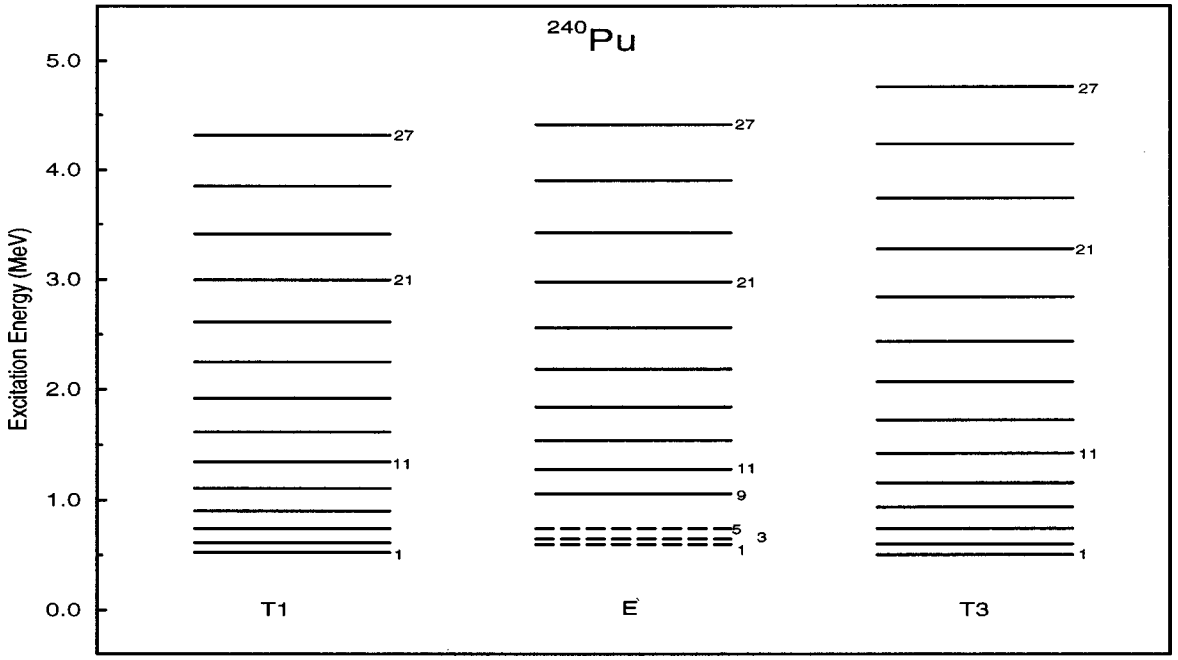

FIG. 8. Comparison of energies calculated using potentials $T1$ and $T3$ with experiment for the lowest band of negative parity states in ^{240}Pu.

^{242,244}Pu in particular, are much smaller than our calculated values (see Table III). We remark further on this point in the next section.

E. ^{244}Cm=^{32}Si+^{212}Pb

Although we would like to model the isotopes of Cm in terms of ^{32}Si clusters and Pb cores, we seem to have reached the limits of applicability of such a binary combination in this region. The value of $B(E2\downarrow;2^+\rightarrow 0^+)$ acts as a good indicator of the dominant cluster to be employed in our modeling of the actinide nuclei, and the systematic variations across the different families of isotopes displayed in Table I [and in line with Eq. (5)] suggest that a Si cluster is certainly appropriate for ^{244}Cm. However, the other isotopes of Cm for which measures of $B(E2\downarrow;2^+\rightarrow 0^+)$ are available are ^{246}Cm and ^{248}Cm, where the measured values of 326 ± 4 and 324 ± 4, respectively, are strongly suggestive of Mg clusters, and we do not pursue our investigations in ^{246,248}Cm further here. For ^{244}Cm the available information on energy levels [39] only goes up to 8^+ in the ground state band, and although the $T1$ potential results fit these limited data quite well, they are not severely tested by them. For this nucleus the calculated values of $B(E2\downarrow;2^+\rightarrow 0^+)$ and $B(E3\uparrow;0^+\rightarrow 3^-)$ are in good agreement with the corresponding measurements (see Tables I and II). However, we predict a large value for $B(E4\uparrow;0^+\rightarrow 4^+)$ whereas no such result is deduced from Coulomb excitation, where a value of zero seems to be consistent with the scattering (see Table III). As for ^{238}U and $^{238-244}$Pu, we thus find a marked discrepancy with $B(E4)$ values deduced from Coulomb scattering for ^{244}Cm. Other (more directly measured) observables for these heavy nuclei are in good agreement with our model predictions, and we strongly recommend confirmation of the $B(E4)$ experimental results.

IV. SYSTEMATIC TRENDS

Our aim in the preceding sections has been to describe the properties of sequences of isotopes ranging from ^{220}Ra to ^{244}Cm as cluster-core combinations interacting through a potential with a fixed prescription. This approach has been quite successful in describing the energies of the lowest bands of states and observed electromagnetic properties. However, there are indications of systematic deviations from experiment.

Our theoretical description of the spectra of the various nuclei examined is good, but not perfect, showing that the shape of the potential we have used could be improved. In particular the 0^+-2^+-4^+ and 1^--3^--5^-, spacings are often calculated to be smaller than those observed, implying that the shape near the origin needs modification. This is particularly true for Ra, less so for Pu, and hardly a problem at all for Th and U.

Another trend in the spectra is that, using the potential prescription of Eqs. (2)–(4), we tend to stretch out the spectra of the lightest nuclei and compress too much those of the heaviest nuclei. This can be corrected by taking the diffuseness of the potential to increase marginally with increasing cluster mass, as can be seen from the better fits obtained with the potential parameters of Eq. (10), where $a=0.77$ fm for the Pu isotopes (Mg clusters). This trend should be reproduced to some extent by a double-folding procedure, involving a core of fixed mass and cluster of increasing mass.

Apart from this feature, there is also a tendency for the spectra of a sequence of isotopes to become more compressed as the mass number increases. This was pointed out for the Ra isotopes, by reference to the energies of their 20^+ states, but is true for the other isotope sequences as well. The trend is captured semiquantitatively by our calculations. Part of this change is certainly due to the increasing effective mass produced by the rising mass number of the Pb core. However, it is also noticeable that the Q value for separating the parent into cluster and core decreases as the Pb-core mass number increases. For our fixed potential geometry prescription this means that the potential radius parameter, obtained by fitting to the Q value, must increase. The larger radius is then responsible for slightly more compressed spectra.

One final note on the spectra is that the observed excitation energy of the bandhead of the lowest 0^- band has a minimum of around 200 keV in ^{222,224}Ra, rising to about 1 MeV in ^{244}Pu. We find that a potential fitted to the properties of a 0^+ ground state band results in the corresponding lowest 0^- bands being several MeV too high. To remedy this, as well as to obtain agreement with the $B(E3\uparrow;0^+\rightarrow 3^-)$ values, we have assumed the potential to be parity dependent. We thus use a different potential depth for the negative parity band (96.5% of that used for the positive parity band) and fit the corresponding radius parameter to the excitation energy of the 5^- state of the negative parity band. This results in a somewhat larger potential radius for the negative parity band than for the positive parity band and has the consequence of compressing the calculated negative parity band a little more than the positive parity band, as if it had a slightly larger effective moment of inertia. This slight compression of the negative parity states with respect to their positive parity counterparts is discernible in the data.

The most striking trend in our results is the sequence of discrete jumps in the values of $B(E2\downarrow;2^+\rightarrow 0^+)$ from one isotope set to another. These are calculated from Eq. (5), where it is found that the value of $\langle r^2\rangle^2$ only changes slightly from one nucleus to another. Thus the $B(E2\downarrow)$ jumps mirror the corresponding jumps in values of $\alpha_2^2\approx[Z_1/(1+A_1/A_2)]^2$ as the cluster charge Z_1 changes from one isotope set to another. The experimental value of $B(E2\downarrow;2^+\rightarrow 0^+)$ therefore gives a very strong clue as to the charge of the cluster to be used in our model, and provides one of the most striking vindications of its applicability in this mass region. Table I shows that a good account can be given of the 18 measured values from ^{220}Ra to ^{244}Cm using a small effective charge of $0.2e$. We have no such simple indication of the mass of the cluster, but a Z/A ratio for a cluster rather similar to that for the core is necessary to avoid an unacceptably large intrinsic electric dipole moment of the cluster-core system. In view of the near constancy of $\langle r^2\rangle^2$, the variation of $B(E2\downarrow;L^+\rightarrow(L-2)^+)$ is closely given by the explicit L dependence shown in Eq. (5). This is well borne out by those few cases where sufficient data exist to check it, i.e., ^{226}Ra [8], ^{232}Th, and ^{234,236,238}U [9].

In all probability, our model should be extended to deal with a linear superposition of different cluster-core combinations centered around the unique pair that we have used to

analyze the data on the actinide nuclei here. In long sequences of isotopes we might then look for evidence of the dominant cluster shifting with changing mass. The lighter isotopes of thorium ($A=222$ and 224) can be best described by ^{14}C clusters orbiting Po cores, a subject which we have not pursued in the present investigation. Rather more surprisingly, the $E2$ data for the heavier isotopes of Cm ($A=246$ and 248) can be best described in terms of Mg clusters orbiting Po cores. There are also indications from exotic decay of the need to introduce a multicluster description; ^{234}U is observed to emit both Ne and Mg ions, and ^{238}Pu emits both Mg and Si ions (for a recent review, see Ref. [40]).

Our model predicts a similar behavior for the $B(E4\uparrow;0^+\rightarrow4^+)$ values, varying as $\alpha^2_{\lambda=4}$. Values inferred from Coulomb excitation experiments are available for 11 of the nuclei we have examined (see Table III). We emphasize that these values are not themselves measured directly, but deduced as necessary input ingredients to a code which seeks to provide a complete description of the Coulomb excitation process. Many of the measured values have considerable error bars, but we can claim that six of them are more or less consistent with the predicted trend. However, the quoted values for ^{238}U and ^{242,244}Pu are significantly smaller than expected (although, again, with large error bars). It should be pointed out that the sign of the $E4$ matrix element is ambiguous, and that if Bemis *et al.* [30] had made a different choice, they would have calculated a much larger value for $B(E4\uparrow;0^+\rightarrow4^+)$. They rejected this choice partly on the grounds that they considered the resulting β_4 deformation parameter to be unreasonably large. We, on the contrary, predict that the β_4 deformation should indeed be very large, and strongly urge a reevaluation of existing Coulomb excitation data and a remeasurement of the heavier nuclei to determine whether the apparent falloff in $B(E4\uparrow)$ is a real effect or not [41].

The $B(E3\uparrow;0^+\rightarrow3^-)$ transition rates and the need for a small parity dependence in the cluster-core potential were discussed in our previous study of the uranium isotopes [9]. Table II lists 11 nuclei where measurements have been made, and rather similar values are obtained in all cases. Our calculations are generally in quite good agreement with these values, but to achieve this the potential parity dependence was crucial. With our adopted parity dependence, we calculate shifts of the positions of the positive parity relative to the negative parity wave functions which are similar in magnitude for all isotopes. However, the wave functions for the heavier nuclei have shorter wavelengths, and so this results in larger phase shifts. This results in the values of $\langle r^3\rangle^2$ becoming progressively smaller. In fact, it more than offsets the increase in the factor $\alpha^2_{\lambda=3}$ so that the predicted $B(E3\uparrow;0^+\rightarrow3^-)$ strengths show a slight decrease with increasing mass number. This decrease appears to be present also in the measured values.

V. SUMMARY

We have examined 19 even-even nuclei ($^{220-226}$Ra, $^{226-234}$Th, $^{232-238}$U, $^{236-244}$Pu, and ^{244}Cm) within a local cluster-core model using a fixed prescription, Eqs. (2)–(4), for the effective potential, and a fixed value, $\epsilon=0.2$, of the effective charge. This approach has previously been shown to give a good description of the measured exotic decay half-lives of these nuclei [7]. Here, we have seen that it also gives a good account of the energies and $E2$ electromagnetic transitions of the lowest $J^\pi=0^+,2^+,4^+,\ldots$ and $J^\pi=1^-,3^-,5^-,\ldots$ bands of states. Experimentally, there is a tendency for the bands of states to become more compressed with increasing total mass than our calculations with fixed parameter values suggest. This can be accommodated within our model by a small increase in the diffuseness of the potential with increasing total mass.

The striking changes in the values of $B(E2\downarrow;2^+\rightarrow0^+)$ observed between one sequence of isotopes and another is naturally explained in our model by a change of cluster charge. Indeed, this feature is so pronounced that it can be used as a strong indication of the charge of the cluster to be employed in any attempt to model actinide nuclei. Similar strong changes of $B(E4\uparrow;0^+\rightarrow4^+)$ are expected from one set of isotopes to another, but are not observed in the currently accepted values for the heavier actinide nuclei ^{238}U, $^{238\text{-}244}$Pu, and ^{244}Cm.

Overall, a good description of the observations on 19 heavy nuclei has been given in terms of a simple binary cluster model. More detailed descriptions in terms of a linear superposition of such cluster-core pairs and through internal excitation of the cluster or core or both are expected to be highly instructive.

ACKNOWLEDGMENTS

A.C.M. and S.M.P would like to thank the U.K. Engineering and Physical Science Research Council (EPSRC) for financial support. S.M.P. would also like to thank the S.A. Foundation for Research and the University of Cape Town for financial support.

[1] B. Buck, A.C. Merchant, and S.M. Perez, Phys. Rev. C **45**, 2247 (1992).
[2] B. Buck, A.C. Merchant, and S.M. Perez, At. Data Nucl. Data Tables **54**, 53 (1993).
[3] B. Buck, A.C. Merchant, and S.M. Perez, Phys. Rev. C **51**, 559 (1995).
[4] B. Buck, J.C. Johnston, A.C. Merchant, and S.M. Perez, Phys. Rev. C **52**, 1840 (1995).
[5] B. Buck, J.C. Johnston, A.C. Merchant, and S.M. Perez, Phys. Rev. C **53**, 2841 (1996).
[6] B. Buck, A.C. Merchant, and S.M. Perez, J. Phys. G **20**, 351 (1994).
[7] B. Buck, A.C. Merchant, and S.M. Perez, Phys. Rev. Lett. **76**, 380 (1996).
[8] B. Buck, A.C. Merchant, and S.M. Perez, Nucl. Phys. **A617**, 195 (1997).
[9] B. Buck, A.C. Merchant, and S.M. Perez, Nucl. Phys. **A625**, 554 (1997).
[10] K. Varga, R.G. Lovas, and R.J. Liotta, Phys. Rev. Lett. **69**, 37 (1992).

[11] K. Varga, R.G. Lovas, and R.J. Liotta, Nucl. Phys. **A550**, 421 (1992).
[12] F. Hoyler, P. Mohr, and G. Staudt, Phys. Rev. C **50**, 2631 (1994).
[13] S. Ohkubo, Phys. Rev. Lett. **74**, 2176 (1995).
[14] S.G. Cooper and R.S. Mackintosh, Inverse Probl. **5**, 707 (1989).
[15] J.C. Johnston, Ph.D. thesis, University of Oxford, 1996 (unpublished).
[16] J.F.C. Cocks *et al.*, Phys. Rev. Lett. **78**, 2920 (1997).
[17] A. Artna-Cohen, Nucl. Data Sheets **80**, 157 (1997).
[18] Y.A. Akovali, Nucl. Data Sheets **77**, 271 (1996).
[19] A. Artna-Cohen, Nucl. Data Sheets **80**, 227 (1997).
[20] Y.A. Akovali, Nucl. Data Sheets **77**, 433 (1996).
[21] H.J. Wollersheim, H. Emling, H. Grein, R. Kulessa, R.S. Simon, C. Fleischmann, J. de Boer, E. Hauber, C. Lauterbach, C. Schandera, P.A. Butler, and T. Czosnyka, Nucl. Phys. **A556**, 261 (1993).
[22] A. Artna-Cohen, Nucl. Data Sheets **80**, 723 (1997).
[23] Y.A. Akovali, Nucl. Data Sheets **69**, 155 (1993).
[24] M.R. Schmorak, Nucl. Data Sheets **63**, 139 (1991).
[25] Y.A. Ellis-Akovali, Nucl. Data Sheets **40**, 523 (1983).
[26] S.P. Tretyakova, A. Sandulescu, V.L. Mikheev, D. Hasegan, A. Lebedev, Yu.S. Zamyatnin, Yu.S. Korotkin, and B.F. Myasoedov, JINR Report No. 7, 1985 (unpublished), p. 23.
[27] E.N. Shurshikov, Nucl. Data Sheets **53**, 601 (1988).
[28] B. Buck, A.C. Merchant, and S.M. Perez, Phys. Rev. C **57**, R2095 (1998).
[29] R.H. Spear, At. Data Nucl. Data Tables **42**, 55 (1989).
[30] C.E. Bemis, Jr., F.K. McGowan, J.L.C. Ford, Jr., W.T. Milner, P.H. Stelson, and R.L. Robinson, Phys. Rev. C **8**, 1466 (1973).
[31] H. Ower, Th.W. Elze, J. Idzko, K. Stelzer, E. Grosse, H. Emling, P. Fuchs, D. Schwalm, H.J. Wollersheim, N. Kaffrell, and N. Trautmann, Nucl. Phys. **A388**, 421 (1982).
[32] E. Grosse, A. Balanda, H. Emling, F. Folkmann, P. Fuchs, R.B. Piercey, D. Schwalm, R.S. Simon, H.J. Wollersheim, D. Evers, and H. Ower, Phys. Scr. **24**, 337 (1981).
[33] B. Ackermann, H. Baltzer, C. Ensel, K. Freitag, V. Grafen, C. Günther, P. Herzog, J. Manns, M. Marten-Tölle, U. Müller, J. Prinz, I. Romanski, R. Tölle, J. deBoer, N. Gollwitzer, and H.J. Maier, Nucl. Phys. **A550**, 61 (1993).
[34] F.K. McGowan and W.T. Milner, Nucl. Phys. **A571**, 569 (1994).
[35] D. Ward, H.R. Andrews, G.C. Ball, A. Galindo-Uribarri, V.P. Janzen, T. Nakatsukasa, D.C. Radford, T.E. Drake, J. DeGraaf, S. Pilotte, and Y.R. Shimizu, Nucl. Phys. **A600**, 88 (1996).
[36] E.N. Shurshikov and N.V. Timofeeva, Nucl. Data Sheets **59**, 947 (1990).
[37] G. Hackman *et al.*, Phys. Rev. C **57**, R1056 (1998).
[38] E.N. Shurshikov, M.L. Filchenkov, Yu.F. Jaborov, and A.I. Khovanovich, Nucl. Data Sheets **45**, 509 (1985).
[39] E.N. Shurshikov, Nucl. Data Sheets **49**, 785 (1986).
[40] E. Hourany, in *Nuclear Decay Modes*, edited by D.N. Poenaru (IOP, Bristol, 1996), p. 350; R. Bonetti and A. Guglielmetti, *ibid.*, p. 370.
[41] J.D. Zumbro, E.B. Shera, Y. Tanaka, C.E. Bemis, Jr., R.A. Naumann, M.V. Hoehn, W. Reuter, and R.M. Steffen, Phys. Rev. Lett. **53**, 1888 (1984).